Chromospheric Oscillations in an Equatorial Coronal Hole

Scott W. McIntosh

Universities Space Research Association, Cooperative Program in Space Science, Seabrook, MD 20706

Laboratory for Astronomy and Solar Physics,
NASA Goddard Space Flight Center, Mailcode 682.3, Greenbelt, MD 20771

scott@grace.nascom.nasa.gov

and

Bernhard Fleck

European Space Agency, Research and Scientific Support Department,
NASA Goddard Space Flight Center, Mailcode 682.3, Greenbelt, MD 20771

bfleck@esa.nascom.nasa.gov

and

Theodore D. Tarbell

Lockheed Martin, Solar and Astrophysics Laboratory,
3251 Hanover Street, L9/41, Building 252, Palo Alto, CA 94304

tarbell@lmsal.com

ABSTRACT

We discuss the appearance and behavior of chromospheric oscillations in and around an equatorial coronal hole as observed by the *Transition Region and Coronal Explorer* (*TRACE*). Phase difference and travel-time analyses of the oscillations in the propagating part of the wave spectrum (6-9 mHz) suggest a significant change in atmospheric conditions at the base of the chromosphere inside the coronal hole relative to its boundary and quiet Sun regions.

Subject headings: solar: chromosphere - solar: atmospheric motions

1. Introduction

Coronal holes are the lowest density plasma components of the Sun's outer atmosphere. They are associated with rapidly expanding magnetic fields, a multitude of wave phenomena and are the seat of the fast solar wind (see the recent review of Cranmer 2002). The low plasma density in coronal holes and the resulting dark signature in coronal extreme ultraviolet (EUV) images would imply that the stratification of the plasma inside the coronal hole is significantly different to that outside of it. Likewise, the magnetic field topology in and around any coronal hole is a delicate, but pervasive, balance of largely "open" field that is surrounded by "closed" field structures on many spatial scales.

Recent investigations of chromospheric oscillations observed by the *Transition Region and Coronal Explorer* (*TRACE*; Handy et al. 1999) and the *Solar and Heliospheric Observatory* (*SOHO*; Fleck et al.

1995) have demonstrated that the structure and strength of the underlying magnetic field significantly alter and inhibit the observed wave fields (e.g., McIntosh et al. 2001; McIntosh & Judge 2001; McIntosh et al. 2003; McIntosh & Smillie 2004). From the preceding statement and opening paragraph of this Letter it would seem natural that a coronal hole presents a topologically obvious place to study chromospheric oscillations at the interface between "open" and "closed" regions of the solar atmosphere.

In the following section we will present *TRACE* observations of chromospheric oscillations in an equatorial coronal hole region. We will then, in Sect. 3, discuss their analysis and the implications of the derived diagnostics on the chromospheric plasma topography just above the temperature minimum at the root of the solar wind.

2. Data & Analysis

We present *TRACE* timeseries data in the 1700Å and 1600Å ultraviolet (UV) continua bandpasses with a 12s cadence[1] observed 2003 July 14 commencing at 00:09UT (ending 01:19UT). Our need to consistently analyze the same spatial region across the bandpasses at full *TRACE* spatial resolution (0.5 arcsec^2) means that the timeseries data for each bandpass must have the effects of solar rotation removed and be carefully coaligned. To this end we employ the *TRACE* Interactive Data Language routine "tr_get_disp_2d.pro" image correlation procedure that is discussed in Krijger et al. (2001) and McIntosh et al. (2003). Context for the *TRACE* observations is provided by the *SOHO* Extreme Ultraviolet Imaging Telescope (EIT; Delaboudiniere 1995) 195Å image taken at 00:08UT that appears in Fig. 1. The *TRACE* field-of-view (FOV) is shown as the thick red rectangular region while the yellow and orange contours represent the 100 and 200 Data Number (DN) intensity levels of the EIT image respectively. These contour levels qualitatively designate the coronal hole boundary.

In Fig. 2 we show the 1700-1600Å phase-difference gradient ($M_{\Delta\phi}$; McIntosh et al. 2003; McIntosh & Fleck 2003) map for the 2003 July 14 dataset. Also shown in this figure are the corresponding locations of the EIT 100 and 200 DN intensity levels (again, as the thick yellow and orange contours) and the black (negative) and white (positive) closed contours of *SOHO* Michelson Doppler Imager (MDI; Scherrer et al. 1995) longitudinal magnetic field ($B_{||}$) magnitude of 20 Gauss. Clearly, inside the coronal hole the $M_{\Delta\phi}$ map shows consistently large values that can be compared to the (very) quiet Sun example presented in Fig. 6b of McIntosh et al. (2003). Likewise, there is a large contrast between the interior ($< M_{\Delta\phi} > \sim 5$ Deg. mHz^{-1}) and boundary regions ($< M_{\Delta\phi} > \sim 1$ Deg. mHz^{-1}) of the coronal hole. Unfortunately, as discussed in Sect. 3 of McIntosh et al. (2003), $M_{\Delta\phi}$ ($\approx \Delta z/V_{\rm phase}$) is not a unique measure; being a mixture of the vertical separation (Δz) of the two bandpasses and the phase velocity ($V_{\rm phase}$) of the waves modes traveling between them. Therefore, the ambiguous interpretation of Fig. 2 is that, in the interior of the coronal hole, we either have a larger Δz or the phase velocity of the wave modes is lower.

As a more intuitive, but no less ambiguous, alternative to $M_{\Delta\phi}$ we introduce a "travel-time" diagnostic between the two bandpasses (see, e.g., Jefferies et al. 1994, 1997; Jefferies 1998). The travel-time (Δt) at any particular frequency (ν) can be computed at the highest possible spatial resolution[2] by taking the timeseries

[1]We note that the *TRACE* bandpass observations are not simultaneous. The 1700Å image being taken 4 seconds before the 1600Å image, but this is accounted for in the presented analysis.

[2]Travel-time estimation does not need the multi-pixel binning that is required to accurately compute the noise-susceptible $M_{\Delta\phi}$ as discussed in McIntosh & Fleck (2003).

in each bandpass and taking a Gaussian filter, $G(\nu;\delta\nu)$, about ν with a relatively narrow 1/e width ($\delta\nu$). Using the filtered timeseries in each bandpass we construct the signal cross-correlation as a function of the lag-time between the timeseries pairs over a (ν dependant) number of exposures; say ten (120s) for a filter frequency of 7 mHz. By fitting a quadratic curve to the maximum of the resulting cross-correlation function we are able to achieve sub-exposure values of the lag-time. A negative lag-time, as is the common convention, indicates that the signal in the 1700Å bandpass leads that in 1600Å by that amount of time. Hereafter, we will equate this lag-time to the oscillation travel-time[3] and a negative value is indicative of an upward disturbance.

While the same ambiguity exists in the interpretation of $M_{\Delta\phi}$ and Δt, the latter, at a specific frequency, can allow a limited interpretation as the time taken for the wave disturbance to travel from one bandpass and into the other by assuming a fixed (neglecting local magnetic modification) wave phase velocity. So, assuming that the waves we are observing in the 7 mHz (± 1.5 mHz) frequency range are sound waves, then the observed travel-time, $\Delta t \approx \Delta z/V_s$, is directly proportional to the height difference between the two bandpasses, where V_s is the sound speed in the lower chromosphere ($\sim$6 km s^{-1}). In Fig. 3 we show the travel-time map, at full *TRACE* resolution, for the coronal hole region where the color-scale now indicates the travel-time of disturbance. Clearly, there is a notable difference in the time-travel map between the coronal hole interior and exterior. In an effort to quantify this difference we have placed three $50'' \times 50''$ regions in the figure: one in the coronal hole interior (red), another in the coronal hole boundary/exterior (blue) and a third over the EUV arcade visible in the 195Å EIT image (purple).

In Fig. 4 we sample across the eleven filters spanning the frequency space (3mHz to 15mHz) in each of the three regions shown in Fig. 3 plus the average of three regions in the well-studied (very) quiet-Sun 1999 February 26 *TRACE* dataset (green curve; McIntosh & Judge 2001; McIntosh et al. 2003). Each colored curve is comprised of the region mean Δt with vertical error bars indicating the standard deviation of Δt in the region and horizontal error bars indicating the 1/e width of the Gaussian filter. While the four curves match (within the errors) at low and high frequencies there is significant departure in travel-time between the red curve and the others between 5 and 10 mHz, with the most obvious difference being between the red and blue curves; the coronal hole interior and exterior respectively. At 7 mHz the nearly 5 second difference between the curves can be approximated to a difference in Δz of 30 km between the two bandpasses. The green and purple curves effectively match across all frequencies within the errors. This could be associated with the presence of mixed polarity magnetic fields and the inclusion of more closed topological structures in those regions; certainly that is the perception of the quiet Sun regions. The difference between the red and green curves is of interest too. It demonstrates that the mean difference in separation between the 1700 and 1600Å bandpasses in the coronal hole interior and in the very quiet Sun[4] is of the order of 12 km (on a pixel-to-pixel basis it is larger ≈ 24km), a not insignificant fraction of a scale height near the chromospheric temperature minimum ($\sim$100km). This indicates a substantial change in thermodynamic conditions between the coronal hole interior and quiet Sun regions at the base of the chromosphere.

[3]Incidentally, it is trivial to show that the travel-time is equivalent to the phase difference between the two signals at that frequency; $\Delta\phi \sim 2\pi\Delta t/\nu$.

[4]In the quiet-Sun alone we can verify that the typical separation of the continuum bandpasses is of the order 30-40 km (Judge 2004 - Private Communication).

3. Discussion

While trying to study the nature of chromospheric oscillations at the interface between open and closed magnetic topologies we found a quite unexpected and confounding result. In the previous section we saw that, at the formation heights of the TRACE UV continua, the plasma inside a coronal hole has a different stratification from that on the coronal hole boundary and also from the quiet Sun inter-network regions. In the latter case this is a significant fraction of a scale height near the chromospheric temperature minimum. This result poses a challenge/question; *why would the largely hydrodynamic (high plasma-β) coronal hole interior plasma at the base of the chromosphere care about the fact that the magnetic field is open to the interplanetary medium and stratify itself so?* Conventional thinking would assume that the chromosphere should have little knowledge of the topologically open coronal holes above.

However, in what has proceeded we have largely neglected the influence of the photospheric magnetic field on the chromospheric oscillations. So, in an effort to address this we will follow the method provided in Sect. 2 of McIntosh et al. (2003) and construct the plasma-β transition height (βTH) map in the *TRACE* FOV. We do this by extrapolating the co-aligned MDI $B_{||}$ and computing the magnetic pressure ($||\mathbf{B}||/8\pi$). Then, by imposing a simple model atmosphere (e.g., model C of Vernazza et al. 1981) to provide a gas pressure, the βTH is then simply the height in the atmospheric cube where the ratio of the gas and magnetic pressures, the plasma-β, is of order unity. For this particular example, the βTH map is shown in Fig. 5. Drawing comparison between Figs. 3 and 5 we can see that there is a strong correspondence between the general features of both the βTH and Δt maps (cf., Fig. 7 of McIntosh et al. 2003), but in particular the regions of high βTH and the longest travel-times at 7 mHz. In fact, it is not a stretch to say that the large travel-times in the coronal hole interior are simply an extension of the inter-network regions shown in McIntosh et al. (2003) where now the magnetic field was weaker and largely unipolar. It would appear that the polarity distribution and mixing play and important role in allowing the observer to distinguish a coronal hole from quiet-Sun plasma.

Multiple equatorial and polar coronal hole regions have been observed with the same *TRACE* Inter-Network-Oscillations (INO) observing sequence in 2003 and the early part of this year, that presented is just one example. Connecting the results discussed above and in the previous section with those of Xia et al. (2003), who demonstrated that equatorial coronal hole inter-network regions had strong Doppler (blue) shifts in transition regions lines, poses some further interesting questions that are somewhat beyond the scope of this Letter. In a future paper (McIntosh et al. 2004) we will discuss the travel-time analysis demonstrated in this Letter in detail and advance it to incorporate temporal intermittence in the chromospheric oscillations present (cf., McIntosh & Smillie 2004). In addition, we will study the other coronal hole observations in detail and study any possible connection between the mixture of field polarities, proportion of open/closed magnetic structures, Δt and Δz in coronal hole interiors with the βTH, UV/EUV intensity/Doppler velocity contrast and *in situ* solar wind measurements.

SWM acknowledges the support of the GSFC SDAC and NASA's Living With A Star Program and would like to thank the *TRACE* team for conducting the INO program. We would like to that Stuart Jefferies and the (anonymous) referee for making many useful suggestions on the text. *SOHO* is a project of international cooperation between ESA and NASA. The TRACE project at Lockheed Martin is supported by NASA Contract NAS5-38099. This material is based upon work supported by the National Aeronautics and Space Administration under Grant NNG04GG34G issued under the Sun-Earth Connection Guest Investigator Program.

REFERENCES

Cranmer, S. R. 2002, Space Sci. Rev., **101**, 229

Delaboudinière, J.-P., Artzner, G. E., Brunaud, A. H., et al., 1995, Sol. Phys., **162**, 291

Fleck, B., Domingo, V., Poland, A. I. 1995, *The SOHO mission*, Dordrecht: Kluwer

Handy, B. N., Acton, L. W., Kankelborg, C. C., et al. 1999, Sol. Phys., **187**, 229

Jefferies, S. M., Osaki, Y., Shibahashi, H. et al. 1994, ApJ, **434**, 795

Jefferies, S. M., Osaki, Y., Shibahashi, H. et al. 1997, ApJ, **485**, L49

Jefferies, S. M. 1998, in *New Eyes to See Inside the Sun and Stars*, Eds. F.-L. Deubner et al., in IAU Symposium 185 Proceedings, Kyoto, Japan, 415

Judge, P. G., Tarbell, T. D. & Wilhelm, K. 2001, ApJ, **554**, 424

Krijger, J. M., Rutten, R. J., Lites, B. W., et al. 2001, A&A, **379**, 1052

McIntosh, S. W., Bogdan, T. J., Cally, P. S., et al. 2001, ApJ, **548**, L237

McIntosh, S. W., Judge, P. G. 2001, ApJ, **561**, 420

McIntosh, S. W., Fleck, B., Judge, P. G. 2003, A&A, **405**, 769

McIntosh, S. W., Fleck, B. 2003, To appear in IAU Symposium 219 Proceedings

McIntosh, S. W., Smillie, D. G. 2004, ApJ, **604**, 924

McIntosh, S. W., Fleck, B., Leamon, R. J., Young, C. A. 2004, In preparation

Scherrer, P. H., Bogart, R. S., Bush, R. I., et al. 1995, Sol. Phys., **162**, 129

Vernazza, J. E., Avrett, E. H. & Loeser, R. 1981, ApJS, **45**, 635

Xia, L. D., Marsch, E., Curdt, E. 2003, A&A, **399**, L5

Fig. 1.— *SOHO* EIT 195Å context image from 00:08UT 2003 July 14. The red rectangular region shows the *TRACE* field-of-view while the yellow and orange contours show the 100 and 200 DN intensity levels in the image, respectively.

Fig. 2.— Phase-difference gradient map at 5×5 *TRACE* pixel resolution. The black and white contours respectively indicate 20 Gauss levels of negative and positive *SOHO* MDI longitudinal magnetic field strength respectively. The thick yellow and orange contours show the 100 and 200 DN intensity levels in the image, as shown in Fig. 1

Fig. 3.— Travel-time map at full *TRACE* resolution. The contours on the figure the same as in Fig. 2. The colored rectangles are used to denote regions of coronal hole interior (red), coronal hole boundary/exterior (blue) and coronal hole arcade (purple).

Fig. 4.— Region averaged travel-times as a function of frequency corresponding to the colored regions in Fig. 3 and that from the quiet 1999 February 26 data (green curve).

Fig. 5.— Spatial variation in the altitudes at which the extrapolated plasma-β is of order unity in the TRACE field of view, the βTH (cf. McIntosh et al. 2003). The contours on the figure the same as in Fig. 2.

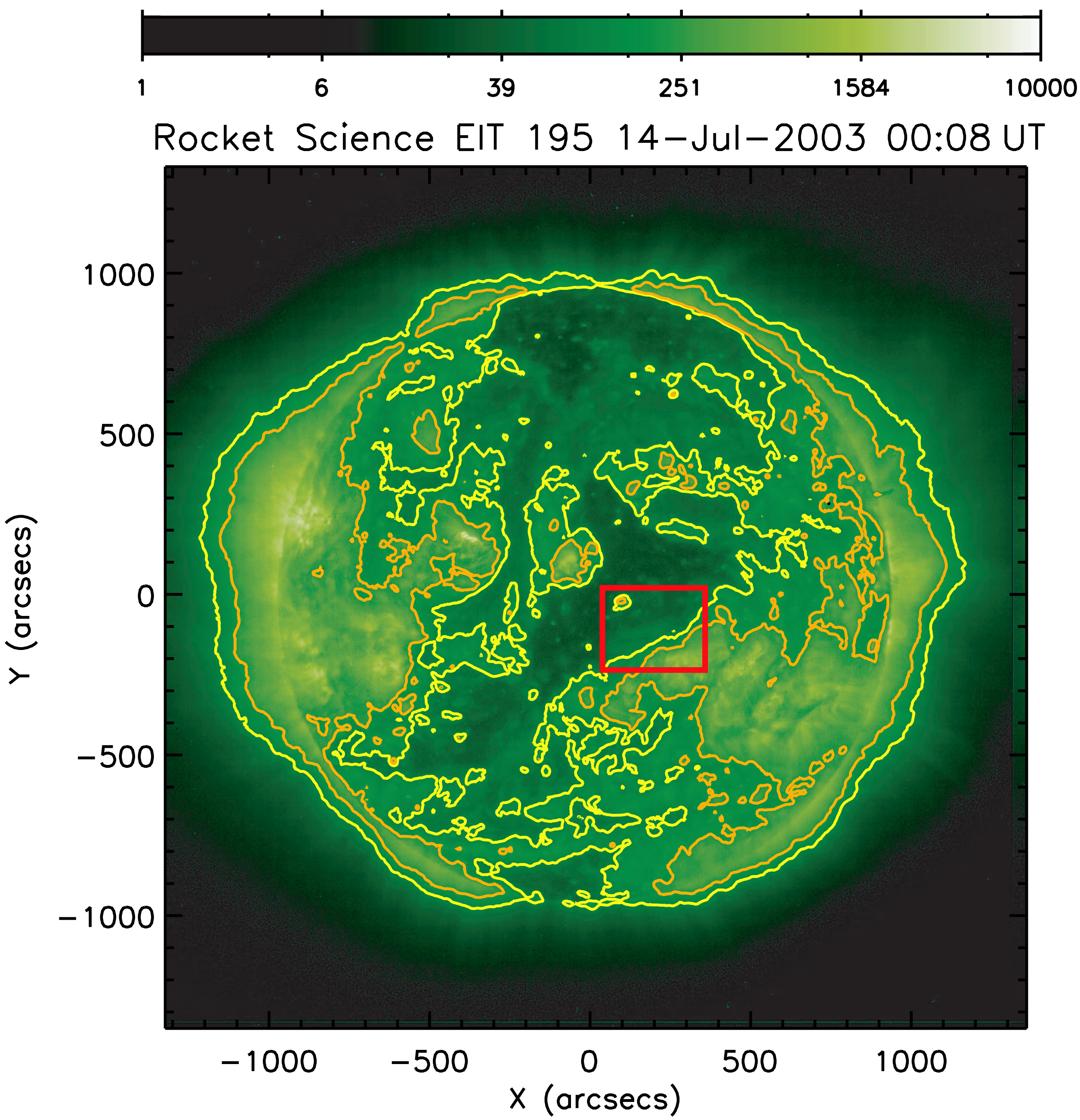
1
6
39
251
1584
10000
Rocket Science EIT 195 14–Jul–2003 00:08 UT
1000
500
0
−500
−1000
Y (arcsecs)
−1000
−500
0
500
1000
X (arcsecs)

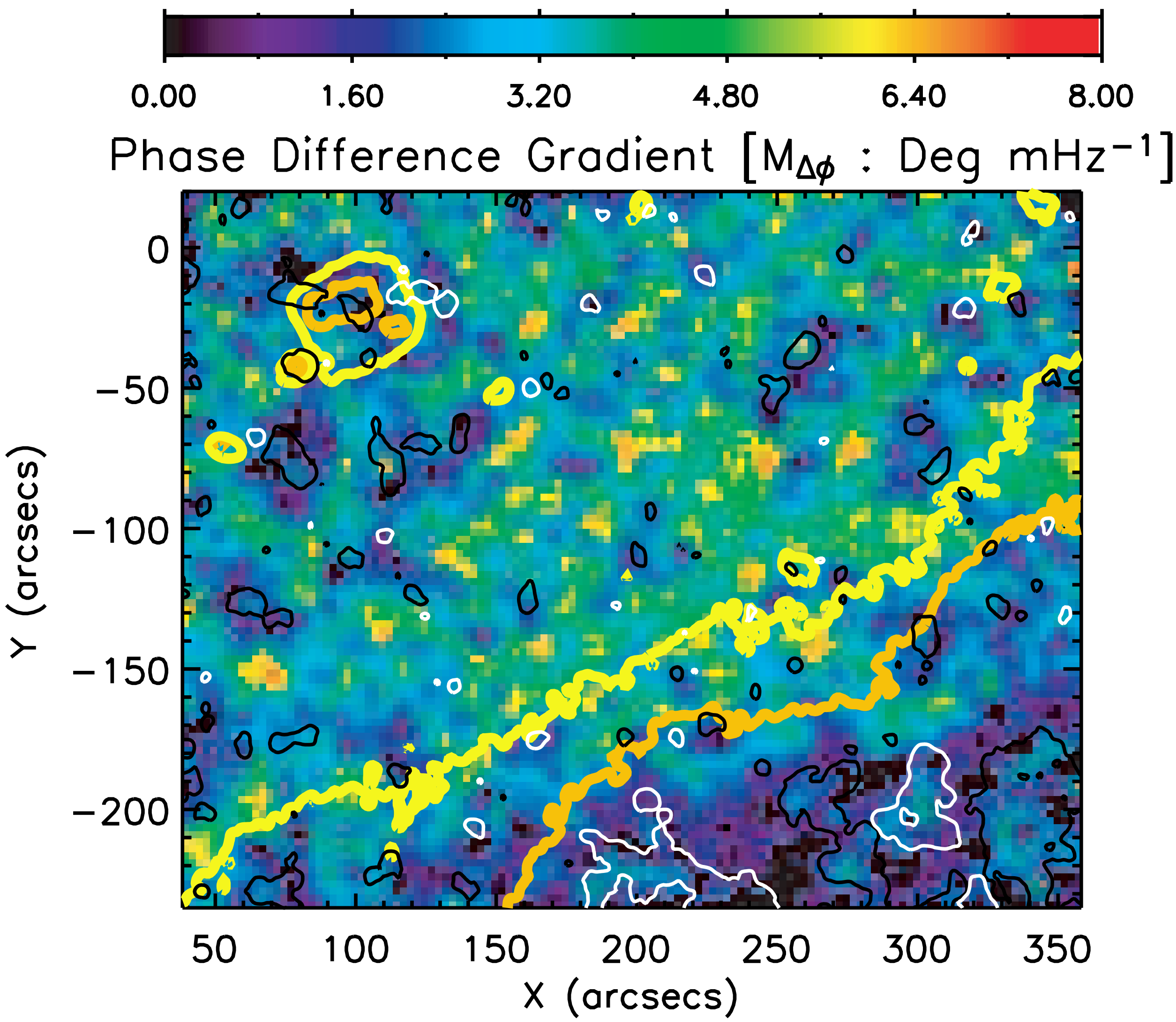
0.00
1.60
3.20
4.80
6.40
8.00
Phase Difference Gradient [$M_{\Delta\phi}$: Deg mHz^{-1}]
0
−50
−100
−150
−200
Y (arcsecs)
50
100
150
200
250
300
350
X (arcsecs)

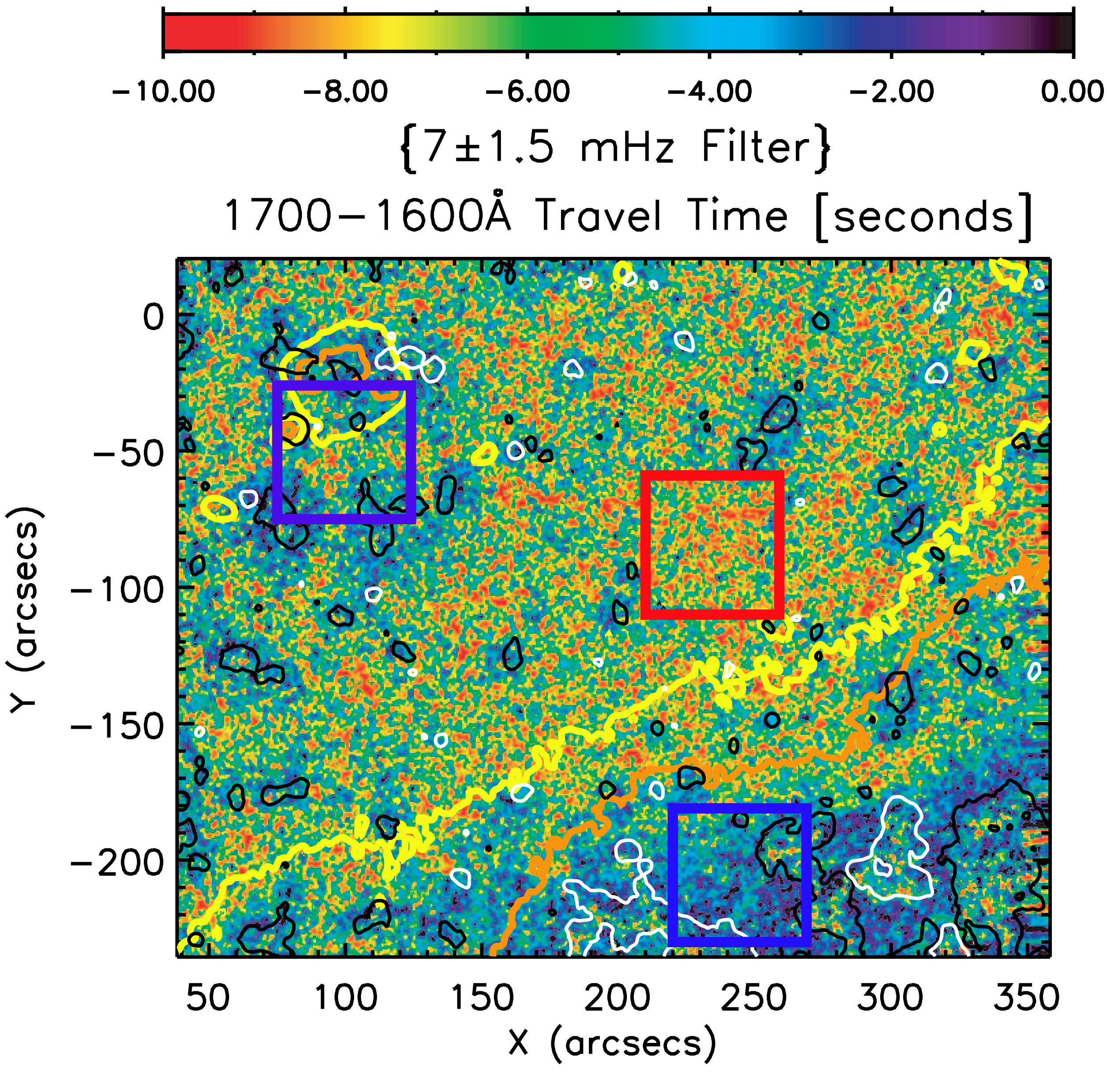
−10.00
−8.00
−6.00
−4.00
−2.00
0.00
{7±1.5 mHz Filter}
1700−1600Å Travel Time [seconds]
Y (arcsecs)
0
−50
−100
−150
−200
50
100
150
200
250
300
350
X (arcsecs)

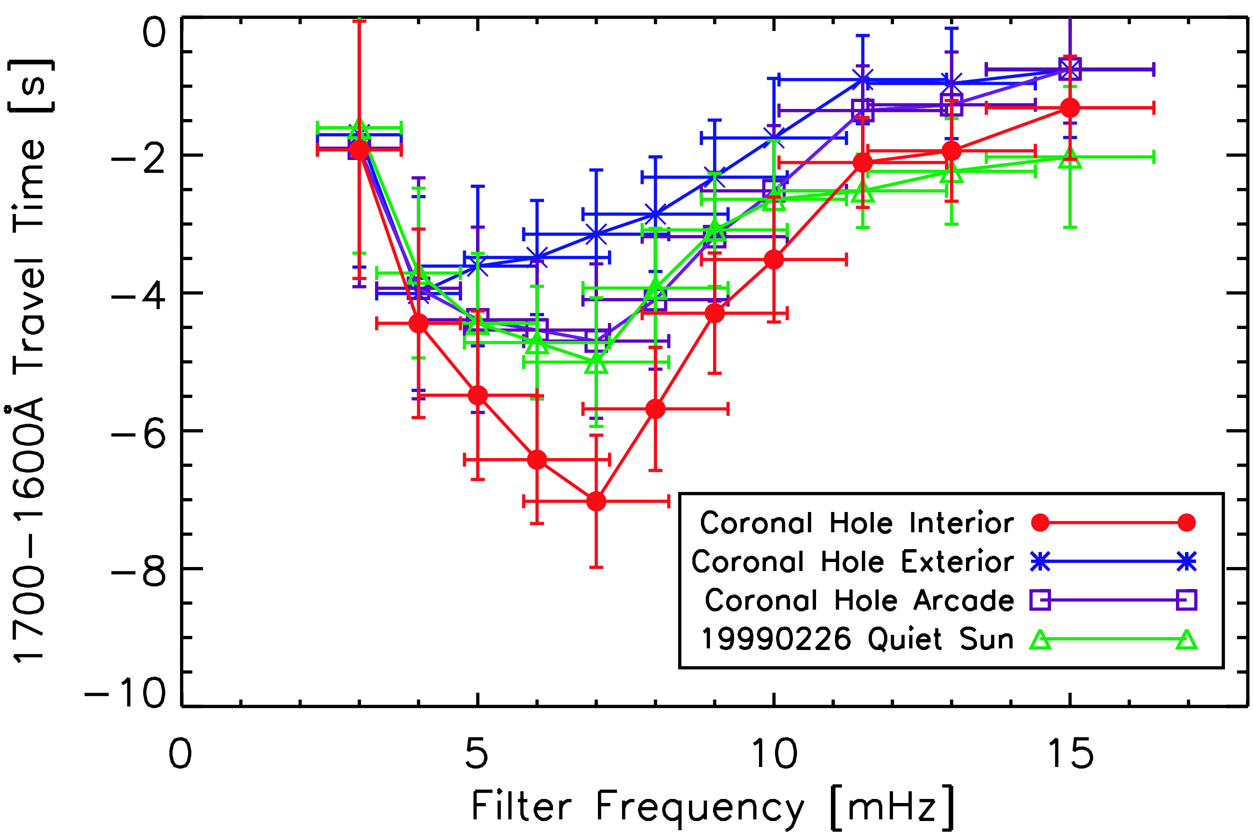

1700−1600Å Travel Time [s]
0
−2
−4
−6
−8
−10
0
5
10
15
Filter Frequency [mHz]
Coronal Hole Interior
Coronal Hole Exterior
Coronal Hole Arcade
19990226 Quiet Sun

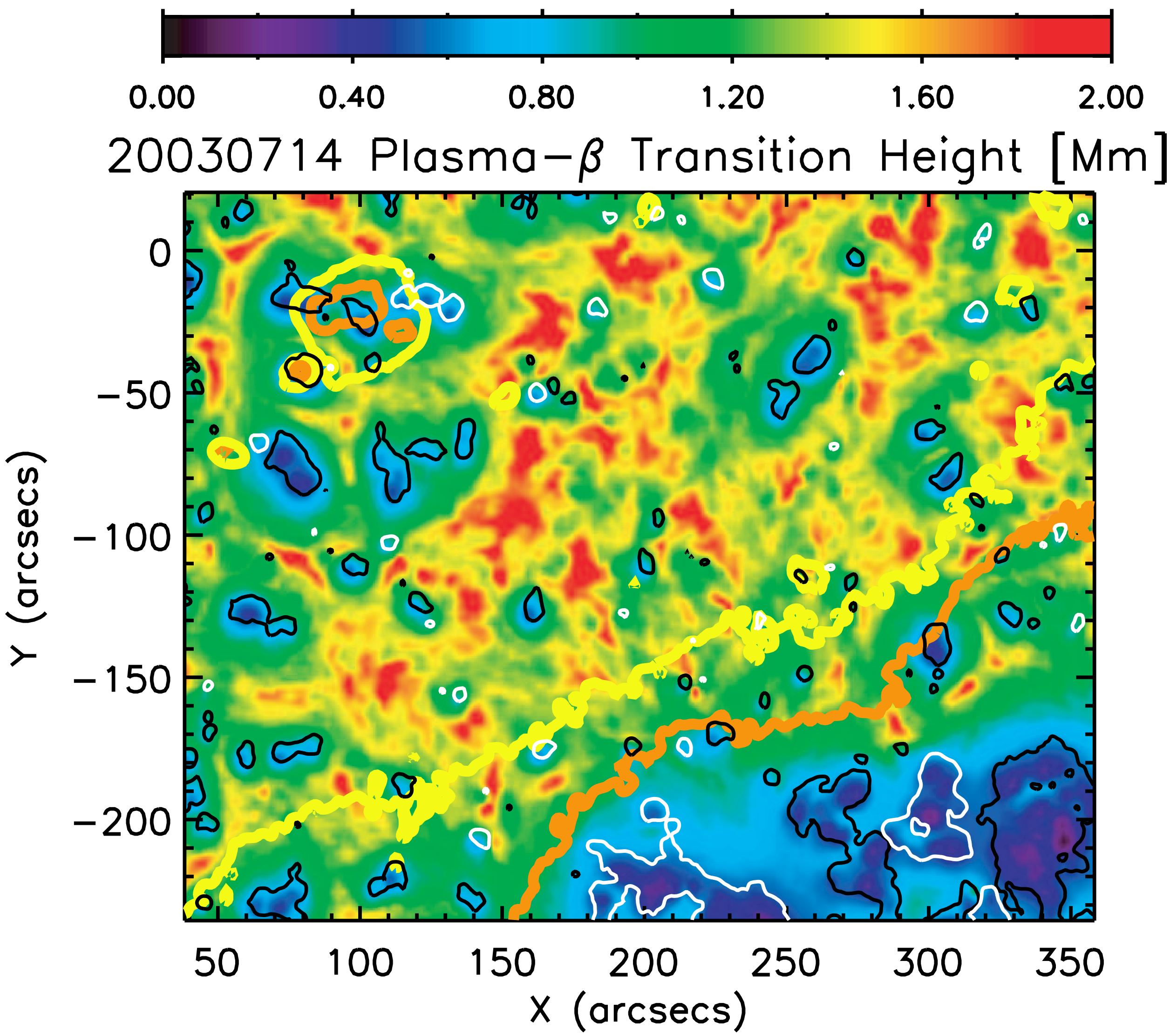
0.00
0.40
0.80
1.20
1.60
2.00
20030714 Plasma−β Transition Height [Mm]
Y (arcsecs)
X (arcsecs)
0
−50
−100
−150
−200
50
100
150
200
250
300
350